Room-Temperature Surface-Erosion Route to ZnO Nanorod Arrays and Urchin-like Assemblies

Zhengquan Li,[a, b] Yue Ding,[b] Yujie Xiong,[b] Qing Yang,*[a, b] and Yi Xie*[a, b]

Abstract: A solution surface-erosion route was successfully employed to produce one-dimensional (1D) ZnO nanostructures. ZnO nanorod arrays and three-dimensional urchin-like assemblies could be selectively obtained with different manipulations. In this process, zinc foil was introduced to an organic solution system and acted both as a reactant and substrate to support the 1D nanostructures obtained. This method, without any template, apparatus, surfactants, or additional heterogenous substrates, has greatly simplified the preparation of oriented 1D ZnO nanostructures. In particular, this simple route could be carried out at room temperature over a period as short as several minutes, thus it could be conveniently transferred to industrial applications. The possible formation mechanism, erosion process, and influence factors were also investigated.

Keywords: nanorods · nanostructures · surface analysis · surface erosion · zinc oxide

Introduction

As a wide-band-gap semiconductor (3.37 eV), ZnO nanomaterials have various applications ranging from surface acoustic wave filters, photonic crystals, light-emitting diodes, photodetectors, photodiodes, and optical modulator wave guides, to varistors, gas sensors, and solar cells.[1] ZnO nanomaterials with one-dimensional (1D) structures, such as nanowires or nanorods, are especially attractive due to their tunable electronic and optoelectronic properties, and potential application in nanoscale devices.[2] Accordingly, various preparative methods have been developed to synthesize 1D ZnO nanostructures for the purpose of obtaining better properties or for applying them to practical use.[3] Among the 1D ZnO nanostructures obtained, well-aligned 1D ZnO nanostructures on substrates seem to exhibit optimal performance, which makes them suitable for the requirements of devices.[2–10] For example, it has been demonstrated that ZnO nanorod arrays on Si substrates can emit an UV or a visible laser at room temperature,[4] and underwent reversible super-hydrophobicity and super-hydrophilicity transitions in UV radiation.[5] Other forms of integrated 1D ZnO nanostructures, such as ZnO nanopropellers on an Al_2O_3 substrates, coral-reef structures on glass, and a hierarchical structures on In_2O_3 nanowires, have also attracted considerable interest and more practical applications are expected.[12]

Several methods have been developed to produce ZnO nanorod arrays, such as chemical vapor deposition (CVD),[6] physical vapor deposition (PVD),[7] metal-organic vapor-phase epitaxy (MOVPE),[8] and anodic aluminum oxide (AAO) templates.[9] Generally, the above-mentioned methods require high temperature or additional templates to act as a support, and they are constrained by expense or apparatus. Comparatively, the solution approach was more attractive for both its simplicity and commercial feasibility, and its good potential for scale-up.[10] Vayssieres et al. developed a wet-chemical method to grow oriented ZnO nanorods on various heterogenous substrates such as Si wafer, F-SnO_2 glass, or single crystalline sapphire.[11] They introduced the heterogenous substrates in a solution system, and then heated the aqueous solution to produce ZnO on the substrates at 95 °C. This "soft" method without any template, apparatus, or surfactants, and so forth, has greatly simplified the preparation of oriented 1D ZnO nanostructures on heterogenous substrates.

Although the orientation of 1D nanostructures on heterogenous substrates has made notable progress, it would seem more convenient if the reactant directly acted as a substrate to support the obtained 1D nanostructures to avoid using an additional substrate. Recently, a high-temperature surface

[a] Dr. Z. Li, Prof. Q. Yang, Prof. Y. Xie
Nanomaterials and Nanochemistry
Hefei National Laboratory for Physical Sciences at Microscale
University of Science and Technology of China
Hefei, Anhui 230026 (P.R. China)
Fax: (+86) 551-360-3987
E-mail: qyoung@ustc.edu.cn
yxielab@ustc.edu.cn

[b] Dr. Z. Li, Y. Ding, Dr. Y. Xiong, Prof. Q. Yang, Prof. Y. Xie
Department of Chemistry
University of Science and Technology of China
Hefei, Anhui 230026 (P.R. China)

 DOI: 10.1002/chem.200400498

reaction method has been developed to synthesize metal oxide/sulfide nanowires on the metal foils through processes such as vapor solid (VS).[13] The surface of the metal foil acts as both the reactant and substrate in this route, which improved the traditional CVD or PVD methods. Low temperature is another desirable synthesis condition that chemists pursue to modify the high-temperature surface-oxidation method. It is thought that when metal foil erodes and produces metal oxide in solution at low temperature, if the formed metal oxide transports to a certain region and then deposits 1D nanostructures on the surface, the metal foil can also act as both a reactant and supporting substrate in solution. Such a solvent surface-erosion method combines the advantages of the "soft" method and high-temperature surface-oxidation method. Furthermore, the experimental procedure can be freely altered in solution at low temperature, thus more than one kind of morphology may be obtained through different manipulations. Based on the above-mentioned consideration, we provide a surface-erosion method to produce differently aligned 1D ZnO nanorods in a solution system. Using this simple process, ZnO nanorod arrays and three-dimensional (3D) urchin-like assemblies were selectively obtained with different manipulations. In particular, this method is carried out at room temperature and is complete in as little as several minutes, thus it is convenient to transfer to industrial applications.

Results and Discussion

Morphologies of ZnO nanostructures on eroded zinc foils: The surface morphologies of zinc foils eroded in both the layered and agitated solution, producing ZnO nanorod arrays and 3D urchin-like assemblies, respectively, were studied by field emission scanning electron microscopy (FESEM). The morphologies of the ZnO nanorod arrays from the layered solution are shown in Figure 1. From the panoramic image (Figure 1a) we can see ZnO nanorods with uniform diameters densely packed and arranged on the surface of zinc foil. The cross-section FESEM image (Figure 1b) shows that these ZnO nanorods grew perpendicularly from the surface of the zinc foil, with diameters around 20 nm and lengths ranging from 200 to 300 nm. It was also found that the substrate was not smooth and that these nanorods were grown from the concave area of the substrate, which indicated that the ZnO nanorod arrays did not grow directly from the surface but from the slightly eroded surface of the zinc foil. On the surface of the zinc foil eroded in the agitated solution, there were many randomly dispersed clusters of 3D urchin-like assemblies. The typical panoramic morphology of a cluster is shown in Figure 2a, which indicates that all the ZnO nanorods aggregated into many separate 3D structures. The magnified FESEM image of a single assembly (Figure 2b) shows that the assembly took on an urchin-like appearance; the diameter of these nanorods was about 30 nm and their length ranged from 300 to 500 nm. The inset image in Figure 2b shows that these nanorods were grown from a rugged substrate on the surface of the zinc foil.

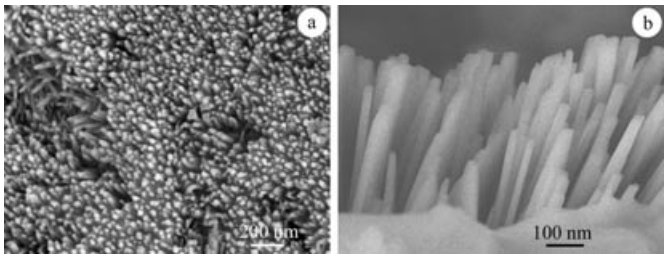

Figure 1. FESEM images of ZnO nanorod arrays: a) panoramic; b) cross-section. The smooth region of the substrate was slightly eroded Zn foil covered by some ZnO.

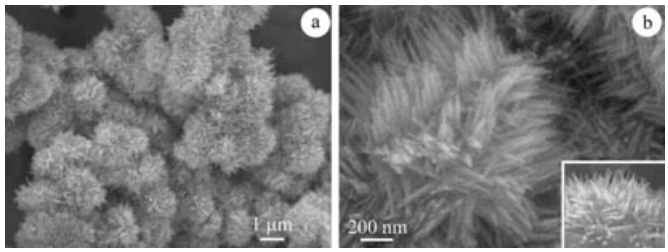

Figure 2. FESEM images of 3D urchin-like assemblies: a) panoramic; b) single 3D assembly.

Phases and purities of both samples

X-ray powder diffraction (XRD) pattern: XRD patterns of sample **a** (nanorods) and sample **b** (urchin-like assemblies) are shown in Figure 3. All the peaks can be clearly indexed to the wurtzite ZnO (JCPDS card No. 36-1451; $a=3.249$, $c=5.206$ Å) and hexagonal Zn (JCPDS card No. 04-0831; $a=2.665$, $c=4.947$ Å). No characteristic peaks were observed for the other impurities, such as $Zn(OH)_2$. The XRD patterns showed that the obtained products only consisted of ZnO and Zn, indicating high purities of the two samples. The peaks of Zn were much stronger than ZnO due to the high proportion of Zn throughout the zinc foils. In the XRD pattern of sample **a**, the relative intensities of peak (002) were stronger than other peaks such as peak (100), which

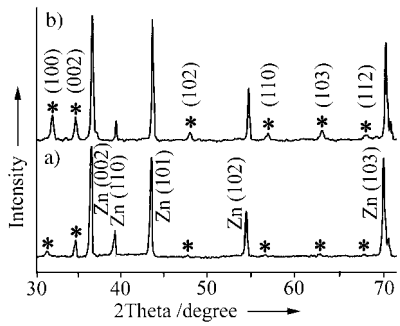

Figure 3. XRD patterns of both samples: a) sample **a**; b) sample **b**. The peaks marked with * belong to ZnO, the others belong to zinc. The peak (101) of ZnO was covered by peak (002) of Zn.

suggests that many ZnO nanorods are oriented along this direction, which is in agreement with their morphologies.

X-ray photoelectron spectra (XPS): XPS of both zinc foils were identified (Figure 4) and confirmed the quality of our products. The binding energies obtained in the XPS analyses

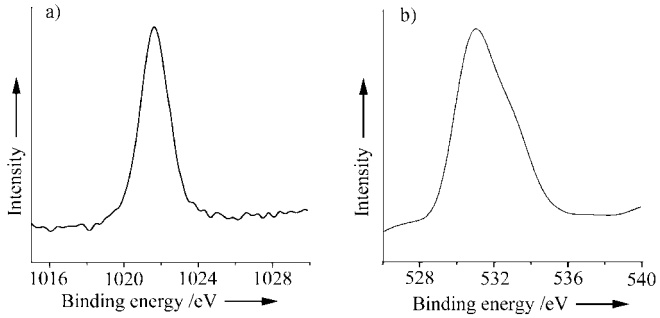

Figure 4. XPS analysis of both samples: a) Zn region; b) O region.

were corrected for specimen charging by referencing the C1s peak to 284.6 eV. In Figure 4a, the peak around 1021.8 eV was attributed to Zn $2p_{3/2}$ of Zn^0 and Zn^{2+} for they have a very close value and integrated together.[14] In Figure 4b, the strong peak at 530.7 eV could be assigned to the O^{2-} in ZnO. No obvious peaks for other elements were observed and the result was in agreement with the XRD patterns.

Photoluminescence (PL) spectra of both samples: The room-temperature PL spectra of samples **a** and **b** are displayed in Figure 5. The excitation wavelength was 325 nm

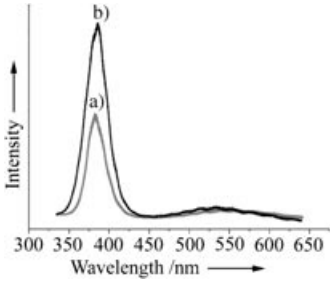

Figure 5. PL spectra of both samples: a) sample **a**; b) sample **b**.

and no filter was used. Strong emission at ~385 nm came from the recombination of excitation centers in the ZnO crystal and the green emission (~520 nm) of ZnO was generally attributed to the recombination of electrons in singly occupied oxygen vacancies with photoexcited holes.[15] The UV peaks in sample **b** were stronger than those in sample **a**, which indicated that more ZnO may be produced in an agitated solution than in a layered solution.

Possible formation mechanism of ZnO nanorod arrays and 3D urchin-like assemblies: In order to obtain ZnO on zinc foil at room temperature, choosing a suitable reaction system seemed to be a crucial factor. Although quite a lot of oxidants in an aqueous system could react with zinc foil at room temperature, Zn^{2+} or $Zn(OH)_4^{2-}$ usually formed in acidic or basic solution, respectively, and no ZnO was deposited on the surface. In our experiment, the organic oxidation solution system consisting of nitrobenzene, methanol, and KOH was found to have the ability to erode zinc foil and form ZnO nanorods on its surface. The overall reaction could be described as shown in Equation (1):[16]

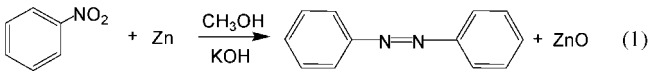

(1)

The redox reaction requires a concentrated basic medium, so methanol was used as a solvent because solid KOH would not dissolve in nitrobenzene. Methanol had the desirable KOH solubility and could be blended with nitrobenzene at any ratio. The half-reactions, (−) and (+), of the redox reaction are shown in Equations (2) and (3), respectively:

$$2\,Zn + 8\,OH^- - 4\,e \rightarrow 4\,Zn(OH)_4^{2-} \quad (2)$$

$$C_6H_5NO_2 + 2\,Zn(OH)_4^{2-} + 4\,e \rightarrow (C_6H_5N)_2 + 8\,OH^- + 2\,ZnO \quad (3)$$

From the half-reactions, one can see that $Zn(OH)_4^{2-}$ was produced from the erosion of zinc foil in solution before it was transported to react with nitrobenzene. ZnO was deposited on zinc foil rather than in solution because the electron was transmitted through the zinc foil during the redox reaction in the organic solution system.

In previous research concerning the formation mechanism of ZnO nanorod arrays on a heterogenous substrate using the "soft" process, it has been demonstrated that a ZnO thin film (or nuclei) initially formed on the substrate before the epitaxial growth.[11] Then, with respect to the structure of wurtzite ZnO, these nuclei would preferentially grow along the (002) direction to form 1D crystals if the chemical environment constantly provided a ZnO resource. As neither templates nor surfactants were used to control the process of crystallization in our experiment, we speculate that the nanorods were formed in an analogous process. In detail, when methanol was saturated with KOH and then mixed with nitrobenzene, two intersaturated phases naturally formed. The upper phase mainly consisted of methanol and KOH, and the lower phase was nitrobenzene. The alkali KOH only participated in the anodic half-reaction, so the zinc foil was well eroded in the methanol phase while slightly eroded in the lower phase. On the other hand, the cathodic half-reaction required the participation of nitrobenzene, thus as $Zn(OH)_4^{2-}$ eroded from the upper phase and constantly diffused to the lower phase, the formation of ZnO nanorods mainly occurred beneath the interface where the concentration of nitrobenzene was higher. The separation of erosion and deposition made the upper phase con-

stantly provide the Zn resource to deposit ZnO onto the region beneath the interface, which is illustrated in Scheme 1a. Therefore, ZnO nanorod arrays could grow epitaxially from the slightly eroded substrate along with the constant transfer of $Zn(OH)_4^{2-}$. Figure 6a shows the morphology of a sample reacted for about one minute. In this figure, the substrate was slightly eroded and coated with immature ZnO nanorods, which confirmed the formation mechanism described above.

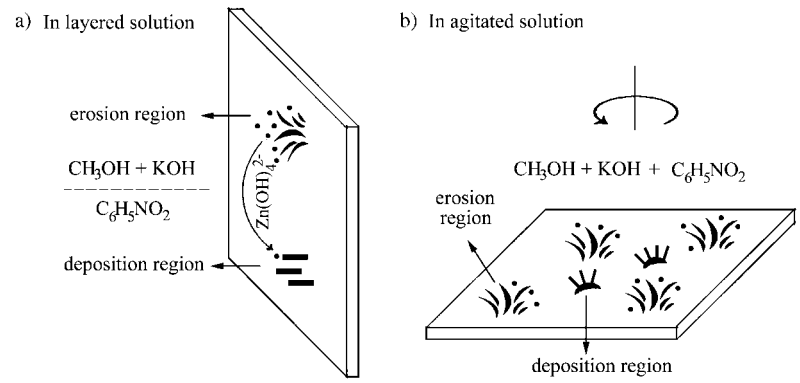

Scheme 1. Illustrations of the formation process of two kinds of morphologies: a) ZnO nanorod arrays; b) 3D urchin-like assemblies.

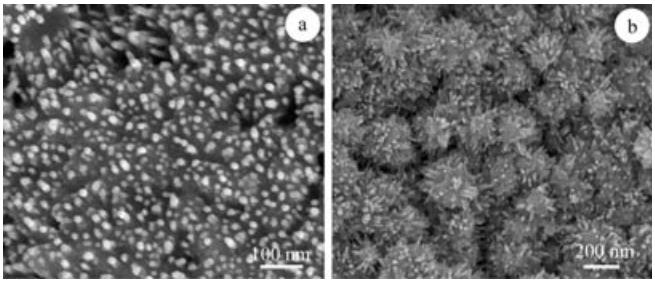

Figure 6. FESEM images of deposition regions in both samples eroded for one minute: a) morphology of sample in layered solution; b) morphology of sample in agitated solution.

Our results have shown that the process of obtaining ZnO nanorod arrays or 3D urchin-like assemblies depended on the procedure used. In an agitated solution, it was no longer possible to set apart the regions of erosion and deposition; the whole zinc foil simultaneously divided into many erosion and deposition regions that alternatively emerged on the whole of the zinc foil. The erosion region provided a ZnO resource to construct ZnO nanorods on the deposition region. But apart from the layered solution, the deposition regions in the agitated solution were uneven because it was well eroded and produced some 3D structures before ZnO nanorods matured. The experimental manipulation of the 3D urchin-like assemblies is illustrated in Scheme 1b. The morphology of the samples eroded for one minute are shown in Figure 6b, revealing the initial stage of these 3D urchin-like assemblies, and providing strong evidence for the 3D urchin-like assemblies growing directly from the eroded surface of the zinc foil.

FESEM studies on the erosion process of zinc foil: In the layered solution, the eroded zinc foil in the methanol phase was also inspected by FESEM and it was found that the different areas of eroded foil exhibited various patterns. This result indicated that the erosion of these areas was not synchronous in all areas. The observed various erosion morphologies could be divided into four distinct types, which are shown sequentially in Figure 7 based on the severity of erosion, indicating the erosion process of the Zn foil. The morphology shown in Figure 7a represents the initial stage of erosion, which showed that shallow pits were formed on the surface and that other areas were left untouched. These pits spread and polyhedral blocks with deep grooves then formed, as shown in Figure 7b. When erosion proceeded, the blocks evolved into individual flake-like crystals with regular shapes, as shown in Figure 7c. For the final step, thinner flakes were carved out and perpendicularly packed to make the rugged landform as seen in Figure 7d. By varying the reaction time, it was found that slight erosion (as shown in Figure 7a, b) dominated the whole surface with a shorter reaction time (<2 min), while the severe erosion (as shown in Figure 7c, d) dominated the whole surface after a longer reaction time (>8 min). No further types of morphology were found even when the reaction time was prolonged to 30 minutes. These comparing experiments confirmed the erosion process of Zn foil described above. In

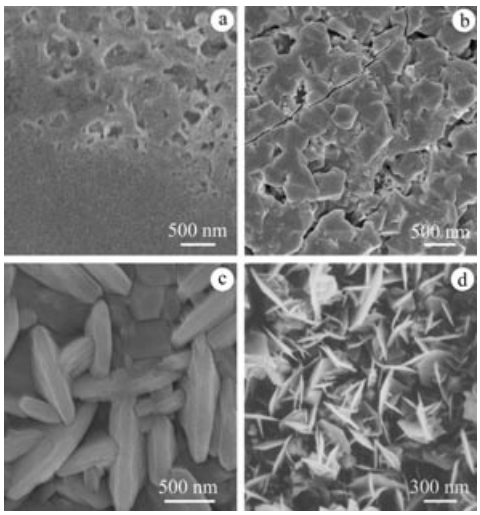

Figure 7. FESEM images of erosion areas of zinc foil with different severity of erosion shown a–d.

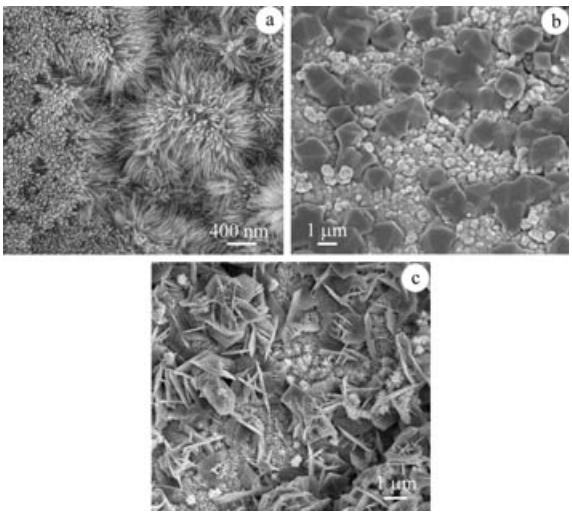

Figure 8. a) Typical FESEM image of deposition region of rough zinc foil eroded for five minutes in layered solution. b) Typical FESEM image of zinc foil eroded for three minutes in agitated solution. c) Typical FESEM image of zinc foil eroded for ten minutes in agitated solution.

the agitated solution, the morphologies of the erosion region on zinc foil were identical to those found in the layered solution.

Influencing factors on the morphology of ZnO nanostructures: It was clear that the difference between the nanorod arrays and 3D urchin-like assemblies was the substrate that these nanorods stood on. So, the key factor in obtaining nanorod arrays was to keep the deposition region on the substrate slightly eroded. Rough substrates or improper manipulation, such as constant shaking, usually produced a hybrid of nanorod arrays and 3D structures (Figure 8a), while the synthesis of 3D structures could be easily achieved regardless of these factors, forming over a long period of time. Figure 8b shows the 3D urchin-like assemblies with a block background obtained after reacting for only three minutes. Figure 8c shows the 3D urchin-like assemblies with a flaky background when the zinc foil was well eroded for ten minutes. While the reaction proceeded, the morphology of the zinc foil remained the same as that shown in Figure 8c.

It has been found that when KOH was replaced by NaOH in our experiment, ZnO nanorods could also be built on zinc foil. But in contrast to the erosion with KOH, ZnO nanorod arrays were formed even if the reaction was carried out in an agitated solution. The surface morphologies of zinc foil eroded for 10 minutes in such a system were investigated by FESEM. Two distinct regions, nanorod arrays (~40%) and erosion regions (~60%) were found to emerge alternatively. Their images are shown in Figure 9a and c, respectively. The ZnO nanorod arrays in Figure 9a appeared like bushes coated on the surface of zinc foil, less densely packed than those obtained with KOH. A magnified FESEM image (Figure 9b) showed these nanorods had a wide size distribution with diameters of about 10–50 nm and lengths of 80–500 nm. Figure 9c shows the eroded regions, which were much different from those obtained with KOH.

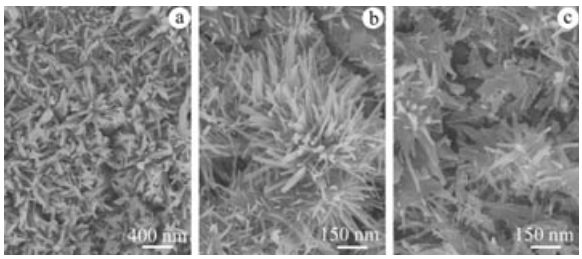

Figure 9. FESEM images of zinc foil eroded for 15 minutes in agitated solution with saturated NaOH: a) panoramic image of deposition region; b) magnified image of deposition region; c) image of erosion region.

In these regions, the substrate was not so severely eroded and ZnO nanorods could still be found. As the erosion continued, the regions of bush-like ZnO nanorods gradually reduced while the eroded regions enlarged, but no 3D urchin-like assemblies or zinc flakes were found. After about one hour, the completely eroded surface remained the same as the erosion areas demonstrated in Figure 9c. NaOH had much weaker alkalescence and about one-third the solubility of KOH in methanol, so the formation of ZnO nanorods required more time. Correspondingly, the severity of erosion was constrained to the initial stage as described in Figure 7a. Since the weak erosion would result in a comparatively slightly eroded substrate, ZnO nanorod arrays could also be built in the agitated solution. Other alkali salts weaker than NaOH, such as Na_3PO_4 or Na_2S could not react with zinc foil and failed to build ZnO nanorods on it. This indicated that strong basic conditions were necessary for this solution surface-erosion process.

Conclusion

In conclusion, a solution surface-erosion route was successfully introduced to produce 1D ZnO nanostructures on zinc foil. ZnO nanorod arrays and urchin-like assemblies could be selectively obtained with different manipulations. This method was carried out at room temperature without any template, apparatus, surfactants, or additional heterogenous substrates. It has greatly simplified the preparation of oriented 1D ZnO nanostructures. The XRD analyses and XPS showed the high purities of the products and the PL spectra indicated their excellent optical properties. The possible formation mechanism was proposed and the erosion process and influence factors were also investigated.

Experimental Section

Syntheses

Surface-erosion process for obtaining ZnO nanorod arrays on zinc foil: Nitrobenzene (30 mL) and methanol (20 mL) saturated with KOH (6.374 g, 0.114 mol) were mixed in a 100 mL beaker, stirred for several minutes, and then stopped to let the solution naturally separate into two phases. Then, zinc foil (6×1 cm) was slowly inserted in the layered solution and kept in touch with both phases for five minutes. The solution was then removed from the beaker and the foil was dried under vacuum

at 80 °C. A piece of eroded foil (1×1 cm) beneath the interface of two phases was cut for further examination (sample **a**).

ZnO 3D urchin-like assemblies: Nitrobenzene (30 mL) and methanol (20 mL) saturated with KOH (6.374 g, 0.114 mol) were mixed in a 100 mL beaker and ceaselessly stirred to blend the two phases. Then, zinc foil (2×2 cm) was thrown into the agitated solution and taken out five minutes later. The foil was dried under vacuum at 80 °C (sample **b**).

Apparatus: FESEM images were taken on a JEOL JSM-6700F SEM. XRD analyses were performed using a Japan Rigaku D/max-χA X-ray diffractometer equipped with graphite monochromatized high-intensity $Cu_{K\alpha}$ radiation ($\lambda = 1.54178$ Å). The accelerating voltage was set at 50 kV, with 100 mA flux at a scanning rate of 0.06 ° s^{-1} in the 2θ range 30–70°. XPS were collected on an ESCALab MKII X-ray photoelectron spectrometer, using non-monochromatized $Mg_{K\alpha}$ X-ray as the excitation source. Room-temperature PL spectra were performed on a LABRAM-HR Confocal Laser MicroRaman Spectrometer equipped with a He-Cd laser.

Acknowledgement

This work is supported by the National Natural Science Foundation of China, Chinese Academy of Sciences, and Chinese Ministry of Education. The authors thank Prof. Fanqing Li for his technical assistance concerning FESEM experiments.

[1] a) N. W. Emanetoglu, C. Gorla, Y. Liu, S. Liang, Y. Lu, *Mater. Sci. Semicond. Process.* **1999**, *2*, 247; b) Y. Chen, D. Bagnall, T. Yao, *Mater. Sci. Eng. B* **2000**, *75*, 190; c) N. Saito, H. Haneda, T. Sekiguchi, N. Ohashi, I. Sakaguchi, K. Koumoto, *Adv. Mater.* **2002**, *14*, 418; d) S. Liang, H. Sheng, Y. Liu, Z. Hio, Y. Lu, H. Shen, *J. Cryst. Growth* **2001**, *225*, 110; e) J. Y. Lee, Y. S. Choi, J. H. Kim, M. O. Park, S. Im, *Thin Solid Films* **2002**, *403*, 533; f) M. H. Koch, P. Y. Timbrell, R. N. Lamb, *Semicond. Sci. Technol.* **1995**, *10*, 1523; g) Y. Lin, Z. Zhang, Z. Tang, F. Yuan, J. Li, *Adv. Mater. Opt. Electron.* **1999**, *9*, 205; h) N. Golego, S. A. Studenikin, M. Cocivera, *J. Electrochem. Soc.* **2000**, *147*, 1592; i) K. Keis, E. Magnusson, H. Lindstrom, S. E. Lindquist, A. Hagfeldt, *Sol. Energy* **2002**, *73*, 51.

[2] a) Z. R. Qiu, K. S. Wong, M. M. Wu, W. J. Lin, H. F. Xu, *Appl. Phys. Lett.* **2004**, *84*, 2739; b) B. P. Zhang, N. T. Binh, Y. Segawa, Y. Kashiwaba, K. Haga, *Appl. Phys. Lett.* **2004**, *84*, 586; c) S. F. Yu, C. Yuen, S. P. Lau, W. I. Park, G. C. Yi, *Appl. Phys. Lett.* **2004**, *84*, 3241; d) Q. X. Zhao, M. Willander, R. E. Morjan, Q. H. Hu, E. E. B. Campbell, *Appl. Phys. Lett.* **2003**, *83*, 165; e) S. Hong, T. Joo, W. I. Park, Y. H. Jun, G. C. Yi, *Appl. Phys. Lett.* **2003**, *83*, 4157; f) W. I. Park, G. C. Yi, J. W. Kim, S. M. Park, *Appl. Phys. Lett.* **2003**, *82*, 4358; g) C. J. Lee, T. J. Lee, S. C. Lyu, Y. Zhang, H. Ruh, H. J. Lee, *Appl. Phys. Lett.* **2002**, *81*, 3648.

[3] a) B. Liu, H. C. Zeng, *J. Am. Chem. Soc.* **2003**, *125*, 4430; b) L. Gao, Y. L. Ji, H. Xu, P. Simon, Z. Wu, *J. Am. Chem. Soc.* **2004**, *126*, 14864; c) Z. R. Tian, J. A. Voigt, J. Liu, B. Mckenzie, M. J. Mcdermott, *J. Am. Chem. Soc.* **2002**, *124*, 12954; d) Z. Q. Li, Y. J. Xiong, Y. Xie, *Inorg. Chem.* **2003**, *42*, 8105; e) Z. Q. Li, Y. Xie, Y. J. Xiong, R. Zhang, W. He, *Chem. Lett.* **2003**, *32*, 760.

[4] a) M. H. Huang, S. Mao, H. N. Feick, H. Q. Yan, Y. Y. Wu, H. Kind, E. Weber, R. Russo, P. D. Yang, *Science* **2001**, *292*, 1897; b) J. H. Choy, E. S. Jang, J. H. Won, J. H. Chung, D. J. Jang, Y. W. Kim, *Adv. Mater.* **2003**, *15*, 1911; c) K. Govender, D. S. Boyle, P. O'Brien, D. Binks, D. West, D. Coleman, *Adv. Mater.* **2002**, *14*, 1221.

[5] X. Feng, L. Feng, M. Jin, J. Zhai, L. Jiang, D. Zhu, *J. Am. Chem. Soc.* **2004**, *126*, 62.

[6] a) J. J. Wu, S. C. Liu, *Adv. Mater.* **2002**, *14*, 215; b) X. Liu, X. H. Wu, H. Cao, R. P. H. Chang, *J. Appl. Phys.* **2004**, *95*, 3141.

[7] a) Y. Zhang, H. B. Jia, R. M. Wang, C. P. Chen, X. H. Luo, D. P. Yu, C. J. Lee, *Appl. Phys. Lett.* **2003**, *83*, 4631; b) Y. C. Kong, D. P. Yu, B. Zhang, W. Fang, S. Q. Feng, *Appl. Phys. Lett.* **2001**, *78*, 407; c) S. C. Lyu, Y. Zhang, C. J. Lee, H. Ruh, H. J. Lee, *Chem. Mater.* **2003**, *15*, 3294.

[8] W. I. Park, D. H. Kim, S. W. Jung, G. C. Yi, *Appl. Phys. Lett.* **2002**, *80*, 4232.

[9] a) Y. Li, G. W. Meng, L. D. Zhang, F. Phillipp, *Appl. Phys. Lett.* **2000**, *76*, 2011; b) C. Liu, J. A. Zapien, Y. Yao, X. Meng, C. S. Lee, S. Fan, Y. Lifshitz, S. T. Lee, *Adv. Mater.* **2003**, *15*, 838.

[10] L. E. Greene, M. Law, J. Goldberger, F. Kim, J. C. Johnson, Y. F. Zhang, R. J. Saykally, P. Yang, *Angew. Chem.* **2003**, *115*, 3139; *Angew. Chem. Int. Ed.* **2003**, *42*, 3031.

[11] a) L. Vayssieres, *Adv. Mater.* **2003**, *15*, 464; b) L. Vayssieres, K. Keis, S. E. Lindquist, A. Hagfeldt, *J. Phys. Chem. B* **2001**, *105*, 3350.

[12] a) P. X. Gao, Z. L. Wang, *Appl. Phys. Lett.* **2004**, *84*, 2883; b) J. H. Choy, E. S. Jang, J. H. Won, J. H. Chung, D. J. Jang, Y. W. Kim, *Appl. Phys. Lett.* **2004**, *84*, 285; c) J. Y. Lao, G. J. Wen, Z. F. Ren, *Nano Lett.* **2002**, *2*, 1287.

[13] a) G. Gu, B. Zheng, W. Q. Han, S. Roth, J. Liu, *Nano Lett.* **2002**, *2*, 849; b) X. C. Jiang, T. Herricks, Y. Xia, *Nano Lett.* **2002**, *2*, 1333; c) Q. Tang, W. J. Zhou, J. M. Shen, W. Zhang, L. F. Kong, Y. T. Qian, *Chem. Commun.* **2004**, 712. d) S. H. Wang, S. H. Yang, *Chem. Mater.* **2001**, *13*, 4794.

[14] a) F. Masanobu, Y. Katsuaki, T. Osamu, *Thin Solid Films* **1998**, *322*, 274; b) B. Mutel, A. B. Taleb, O. Dessaux, P. Goudmand, L. Gengembre, J. Grimblot, *Thin Solid Films* **1995**, *266*, 119.

[15] K. Vanheusden, W. L. Warren, C. H. Seager, D. R. Tallant, J. A. Voigt, B. E. Gnade, *J. Appl. Phys.* **1996**, *79*, 7983.

[16] E. C. Horning, *Organic Syntheses, Collective Vol. 3*, John Wiley & Sons, New York, **1955**, p. 103.

Received: May 20, 2004
Published online: October 7, 2004